Available online at www.sciencedirect.com

ScienceDirect

journal homepage: www.elsevier.com/locate/he

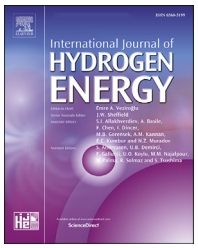

Large-scale underground hydrogen storage: Integrated modeling of reservoir-wellbore system

Mohab Abdellatif [a], *Mehrdad Hashemi* [b], *Siroos Azizmohammadi* [c,*]

[a] *Operations Department, Agiba Oil Company, Cairo, Egypt*
[b] *Vision Advanced Petroleum Solutions LLC, Muscat, Sultanate of Oman*
[c] *Department of Petroleum Engineering, Montanuniversität Leoben, 8700 Leoben, Austria*

HIGHLIGHTS

- Integrated modeling will enhance the predictions.
- The type of cushion gas is crucial for production targets.
- Hydrogen diffusion has a minor impact on a field scale seasonal storage.
- The injection-production strategy will influence production efficiency.

ARTICLE INFO

Article history:
Received 7 November 2022
Received in revised form
18 January 2023
Accepted 19 January 2023
Available online 24 February 2023

Keywords:
Underground hydrogen storage
Depleted gas reservoir
Integrated modeling
Cushion gas
Hydrogen diffusion
Injection-production strategy

ABSTRACT

Underground Hydrogen Storage (UHS) has received significant attention over the past few years as hydrogen seems well-suited for adjusting seasonal energy gaps.

We present an integrated reservoir-well model for "Viking A" the depleted gas field in the North Sea, as a potential site for UHS. Our findings show that utilizing the integrated model results in more reasonable predictions as the gas composition changes over time. Sensitivity analyses show that the lighter the cushion gas, the more production can be obtained. However, the purity of the produced hydrogen will be affected to some extent, which can be enhanced by increasing the fill-up period and the injection rate. The results also show that even though hydrogen diffuses into the reservoir and mixes up with the native fluids (mainly methane), the impact of hydrogen diffusion is marginal. All these factors will potentially influence the project's economics.

Introduction

The impacts of climate change are catastrophic to nature and people, threatening our planet's health and eventually leading to an uncertain future. The latest Intergovernmental Panel on Climate Change (IPCC) [20] explained the impacts of climate change and provided the necessary actions to adapt to such a phenomenon. Unfortunately, as stated in their report, some of these impacts are irreversible. In this context, 196 countries adopted the Paris Agreement [31] to limit global warming below 1.5 °C. Greenhouse gas emission is a direct contributor

* *Corresponding author.*
E-mail addresses: mohab.abdellatif@agiba.com (M. Abdellatif), mehrdad@visionaps.com (M. Hashemi), siroos.azizmohammadi@unileoben.ac.at (S. Azizmohammadi).

https://doi.org/10.1016/j.ijhydene.2023.01.227

to climate change. Therefore, reducing greenhouse gas emissions is the primary measure to mitigate the impact of global warming.

Following the Paris agreement and implementing its articles, the world is gradually transforming from fossil fuels to carbon-neutral ones. Several initiatives have been taken in these regards. Clean energy for all Europeans [5] is one of Europe's vital initiatives to tackle the energy transition to ensure a clean and fair energy transition. They are targeting by 2030 at least a 40% cut in greenhouse gas emissions, 32% renewables in energy consumption, and 32.5% energy efficiency, which in turn will lower the EU's reliance on imported energy, mainly in the form of oil and gas to make the energy supply more secure and fight against any possible blackouts in case of emergencies. However, total reliance on renewable energy sources such as wind and solar is still being researched. As such, energy sources are highly weather dependents, and the electricity produced fluctuates. This fluctuating nature of produced electricity, which does not match the consumption rates, requires a vast energy storage system. From an economic point of view, pumped hydro and compressed air energy systems (CAES) are more economical for smaller volumes of fuel when compared to hydrogen. Still, for more considerable volumes, hydrogen is the better choice [27].

It has been proven that hydrogen can be utilized as an energy carrier to store surplus energy during low energy consumption and regenerate it during high energy consumption.

The underground storage of gases was first introduced in 1915 in a partially depleted gas field in Ontario, Canada [35]. Due to this similarity between UHS and natural gas storage, most of the underground hydrogen storage projects make use of the experience gained from natural gas storage but, of course, considering the physical and chemical differences between hydrogen and natural gas, as hydrogen is more chemically active and has a high affinity for chemical, and microbial reactions underground, in addition to the physical properties of hydrogen such as high diffusivity, low viscosity, and high mobility. All these characteristics make hydrogen storage more complicated as hydrogen is more susceptible to leakage and energy loss [21].

Several studies address the geological and operational impacts of underground hydrogen storage. For an in-depth and comprehensive review of underground hydrogen storage, mechanisms, efficiency, and associated challenges, the interested reader is referred to Refs. [15,30] and the references therein. To highlight some studies: Pfeiffer and Bauer [19] investigated a hypothetical site based on actual geologic data in Schleswig-Holstein, Germany. The aim was to create a storage site to mitigate the energy production gap for one week by optimizing the injection scheme, shut-in periods, and initial filling of the reservoir. Amid et al. [1] worked on Rough Gas Facility to compare its energy output against a case where hydrogen is used as the working gas in that depleted gas reservoir. Phreeqc geochemical modeling tool was used to examine the chemical stability of the pool. Several assemblages of minerals in the presence of hydrogen and water were investigated. Their study showed that Clay-bearing sandstone and iron oxides are stable under the reservoir condition, while the sulfur-containing sample produced H_2S. Therefore, the proper reservoir should be selected that either has little sulfur or is too hot to prevent the chemical activity of hydrogen. In 2010 Hychico [3] looked for a potential UHS in a depleted gas reservoir near its hydrogen facilities. The project aimed to test the reservoir capacity and tightness. Their results show that underground hydrogen storage can involve chemical and microbial reactions and alteration of reservoir characteristics such as permeability. Tarkowski and Czapowski [28] analyzed seven salt domes as promising sites for hydrogen storage, showing the geological conditions favorable for hydrogen storage, and also discussed the advantages of hydrogen storage in depleted reservoirs. Heinemann et al. [10] investigated three conceptual hydrogen storage plays in the Midland Valley of Scotland and assessed their conditions as future potential targets for pilot projects. Hassannayebi et al. [9] studied the geochemical interaction of hydrogen in a depleted gas reservoir in the Molasse Basin in Upper Austria. They proposed a geochemical modeling workflow that results in extensive insight into the contributing mechanisms and risk evaluation in such projects. Their findings show considerable uncertainty in the process due to a lack of experimental and field data. Therefore, the disturbance of reservoir integrity associated with geochemical interactions with hydrogen cannot generally be ruled out, and it is more site-specific that needs particular considerations. Several studies highlighted that microbial reactions initiated by various bacteria and archaea are challenging during underground hydrogen storage [3,6,8,12,29]. These studies showed that such microbial reactions might influence the overall performance of underground hydrogen storage projects. Lemieux et al. [13] assessed possible hydrogen storage in geological formations such as salt caverns, depleted oil and gas fields, and aquifers. Shi et al. [24] studied the impact of storing a mixture of hydrogen and natural gas in an existing natural gas storage site in California and investigated the alteration of the reservoir properties such as permeability, porosity, surface area, mineralogy, and structural characteristics caused by hydrogen injection. Their results show a decrease in caprock permeability after exposure to the gas mixture, indicating an improvement in the sealing capacity. Wang et al. [33] performed a 2D simulation with a very fine cell size to examine the flow behavior of H_2 with CO_2 as a cushion gas. They analyzed the viscous instability, capillary bypassing, gas trapping, and gravity effects. They applied three dimensionless groups to correlate different scales, including aspect ratio, capillary/viscous ratio, and gravity/viscous ratio. Lysyy et al. [14] studied the Norne field and examined three scenarios by injecting pure hydrogen into the gas, oil, and water zones. Their results show that the thin gas zone gives the highest hydrogen recovery factor while the geologic structures and fluid saturation determine the hydrogen distribution. Okoroafor et al. [17] investigated the reservoir, geological, and operational controls that affect large-scale hydrogen storage using the ECLIPSE E300 reservoir simulator. They introduced a screening criterion for potential underground hydrogen storage sites and a methodology to rank geological and reservoir properties.

While most of the simulation studies on underground hydrogen storage utilize conceptual/hypothetical models or/and only consider reservoir simulation, this study elaborates on the effectiveness of integration between the reservoir and

the well models to address the practical application of large-scale underground hydrogen storage. The sensitivity analysis is carried out to examine the role of cushion gas, the impact of hydrogen diffusion, and the effect of injection rate and schedule on the performance of UHS.

This paper proceeds as follows. First, the characteristics of the target field and the required data are reviewed. Second, the different elements used in the modeling step are introduced, and the features are discussed. The simulation results and the respective interpretations of the findings are presented in section 3. The sensitivity analysis of contributing parameters is shown in section 4, followed by conclusions at the end.

Materials and methods

Viking a gas field - UK North Sea

This study considers the Viking A field in the North Sea as a potential hydrogen storage site for the following reasons: (1) Need for electricity: Electrolysis is green carbon-free hydrogen production from renewable resources. There are tens of wind farms currently operating in the North Sea. When writing this paper, Germany, Belgium, the Netherlands, and Denmark pledged to build 150 GW of offshore wind capacity in the North Sea to help achieve the EU's climate goals and, eventually, break away from imported energy [2]. Therefore, it would be helpful to have such an energy buffer or temporary storage in the area to store the energy generated from these wind farms; (2) The availability of data: Viking A is one of the potential sites selected for Carbon Capture and Sequestration (CCS) projects in the UK offshore. There are several publications in this field, and the reservoir model is available for the CCS project [18]; (3) Almost fully depleted reservoir: It is a highly depleted reservoir with more than 90% recovery ceased in 1991. Thus, not much hydrocarbon will be lost.

The Viking field is located in the Southern North Sea, approximately 140 km east of Lincolnshire, in blocks 49/12a, 49/16, and 49/17. The original field contains nine reservoirs (A, B, C, D, E, F, G, Gn, and H). The whole field contains approximately 2990 BCF gas in place of which 2895 BCF has been produced with nearly 97% recovery factor as of December 1999 [22]. A detailed description of the structure and stratigraphy can be found in Refs. [4,23,26,32,34]. Viking A was discovered by well 49/12–2 in March 1969, put into production in October 1972, and ceased in 1991 after production of 1035.42 BCF [16]. Table 1 shows a data summary of the Viking gas fields.

Table 1 – Viking gas fields data summary [22].

Trap	
Type	Tilted/inverted fault blocks
HC contact	Variable 9000–10,200 ft
Gas Column	700 ft max. in the Rotliegendes
Formation	Leman Sandstone Formation
Age	Permian
Reservoir	
Gross thickness	400–700 ft
Porosity	7–25%
Permeability	0.1–100 mD
Water saturation	0.1 average value
Rock Compressibility	9.814×10^{-7} psi^{-1}
Reservoir temperature	183 °F average value
Initial pressure	4150-4670 psi
Current pressure	500 psi average value

The Viking A is considered as one of the potential sites for Carbon Capture and Sequestration (CCS) offshore projects in the North Sea, UK. The reservoir model of the Viking field was initially built by Pale Blue Dot Energy [18] and is available in the public domain. For this study, we extracted RESCUE files from the Eclipse model to import them into the CMG-GEM simulator, where we can simulate hydrogen storage and then integrate reservoir and wellbore models into the CoFlow platform.

Reservoir geometry

Fig. 1 shows the 3D grid and depth map of the Viking A reservoir implemented in CMG.

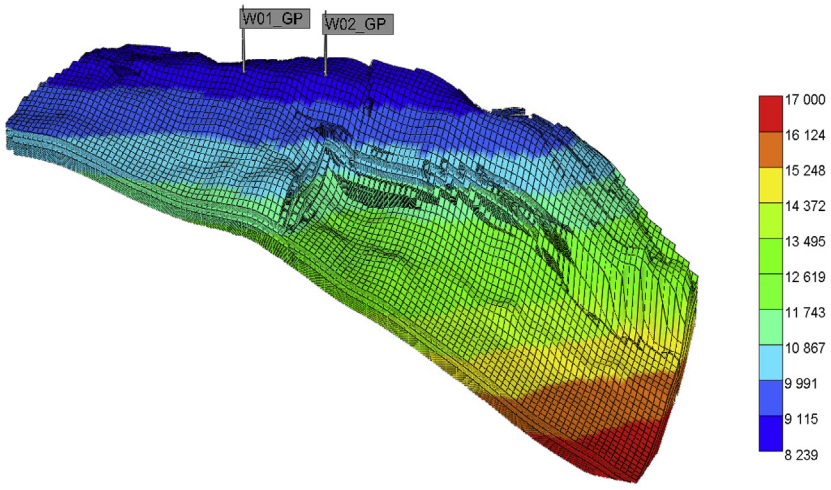

Fig. 1 – The 3D view of the grid and corresponding depth map (units are in ft).

The grid and reservoir properties are directly taken from the RESCUE file exported from the original Eclipse model.

Initial condition

The reservoir pressure, water saturation, and fluid composition are taken from the original Eclipse model, and the model is initialized by enumeration. Table 2 shows the average composition of the fluid.

Table 2 – Average initial composition.

Component	Symbol	Mole Percentage
Methane	C1	90.3
Ethane	C2	4.5
Propane	C3	1.2
Nitrogen	N2	2.8
Others	Others	1.2

Fluid model

The fluid model was created in CMG-WinProp using the PR78 equation of state. WinProp is the PVT modeling tool provided by the CMG simulation package to tune the equation of state for predicting fluid behavior at reservoir conditions. Table 3 shows the list of components used in the fluid model. The reservoir temperature is uniform and set at 183 °F.

Table 3 – The list of components used to create a fluid model.

Component	Symbol	Pc (atm)	Tc (K)
Hydrogen	H2	12.80	33.2
Carbon Dioxide	CO2	72.90	304.7
Nitrogen	N2	33.50	126.2
Methane	C1	45.44	190.6
Ethane	C2	48.20	305.4
Propane	C3	41.90	369.8
Butane	C4	36.98	419.5
Pentane	C5	33.15	465.9
Hexane	C6	29.71	507.5
Heptane	C7	29.00	548.0

Rock-fluid model

The gas saturation in the reservoir varies from 0.7 to 0.95, and the liquid phase is considered an immobile phase in our model.

Injection and production strategy

The operation starts on 01-Jan-2031 by either fill-up or cushion gas injection to pressurize the reservoir such that the wells can produce naturally at the desired production rate. This is followed by five annual hydrogen injection/production cycles until 01-Mar-2037. Hydrogen is injected during summer (March to September), when the electricity demand is low, followed by three months of a shut-in. Then, the stored hydrogen is produced and retrieved during winter (December to March) (see Table 4 below).

Base case

The base case consists of fill-up the reservoir with hydrogen for nine months with an injection rate of 30 MMSCF/day/well, followed by cycling as shown in Table 4. The injection rate and the period for a fill-up are determined after several trials so that the reservoir can produce at a desirable production rate of 40 MMSCF/day/well for three months, double the injection rate of 20 MMSCF/day/well for six months.

Table 4 – Base case strategy.

Event	Period (month)	Rate (MMSCF/day/well)
Fill-up	9	30
Shut-in	3 (Sep–Nov)	–
Production	3 (Dec–Feb)	40
Injection	6 (Mar–Aug)	20

Well model

As shown in Fig. 1, the model has two vertical wells located on the crest of the reservoir, and each well is used as a producer or an injector during different cycling periods. Therefore, two producers and two injectors named W01-GP, W01-GI, W02-GP, and W02-GI are defined in the model.

As pure hydrogen is being injected into the reservoir, a pure hydrogen lift table is required for injectors. However, the produced gas could be a mixture of hydrogen, methane, and a small fraction of the other native gases. Therefore, for producers, two extreme lift tables are defined: (1) the H2 lift table: assuming the produced gas is 100% hydrogen (2) the CH4 lift table: assuming the produced gas is 100% methane.

From a production perspective, a lift table or lift curve demonstrates the flow performance of a well, that is, how much pressure is required to lift a certain amount of fluid to the surface at the given wellhead pressure.

In this work, the lift tables are built using Gray correlation [7] in the PIPESIM (multiphase flow simulator for wells, flowlines, and pipeline systems, including surface equipment). Table 5 shows the well downhole equipment used to setup the well model and generate the lift tables.

The overall heat transfer coefficient of 3 Btu/(hr.ft^2.F) is used for vertical gas flow calculations.

Table 5 – The well downhole equipment.

	Bottom MD (ft)	ID (in)	Wall Thickness (in)	Roughness
Casing	9300	8.681	0.472	0.001
Tubing	8300	4.95	0.275	0.001

Table 6 shows the constraints defined for different periods of injectors and producers in different project phases.

Table 6 – The well constraints defined in the simulation model for different periods.

Phase	Parameter	Value
Fill-up	Well-head pressure	800 (psi)
	Injection rate	30 (MMSCF/day/well)
Hydrogen Injection	Well-head pressure	800 (psi)
	Injection rate	20 (MMSCF/day/well)
Hydrogen Production	Well-head pressure	100 (psi)
	Production rate	40 (MMSCF/day/well)

Standalone model

The standalone model consists of the reservoir model with predefined lift tables, either pure H2 or pure CH4 lift tables, introduced in the previous section. It should be noted that this is an ideal assumption because the produced gas composition changes over time; therefore, the lift tables considering a fixed composition (pure H2 or pure CH4) cannot describe the actual production characteristics.

Integrated model with CoFlow

The integrated Asset Modeling (IAM) tool is commonly used to couple the different production elements (reservoir, well, and surface facility) into a single model, enabling us to examine the impact of individual production components on the total performance of the field.

Each injector has two sources, one for cushion gas (de-activated in the base case as we are filling up with hydrogen) and one for hydrogen for storage cycling and set the properties of the sources to match the base case strategy (the shut-in and start times, flowrate limits, fluid type, etc.). The two producers are connected to a 2-phase separator.

For further analyses, the reservoir, well, rock and fluid models, and well constraints and events are implemented into the CoFlow package.

Simulation results

Here the results of standalone and integrated models are presented to compare the performance of each for underground hydrogen storage.

Standalone model: As can be seen in Fig. 2 (left), the field can produce at the target of 40 MMSCF/day/well (i.e., 80 MMSCF/day in total for two wells) when using a H2 lift table (blue lines). However, this cannot be achieved if a CH4 lift table (yellow lines) is being used. This can be explained by the pressure plot in Fig. 3, where the WHP constraint of 100 psi is violated when using the CH4 lift table. The reason would be that the hydrostatic column in the case of pure methane is much heavier than pure hydrogen case, and consequently, the pressure drop is higher and the production rate is lower. Moreover, Fig. 2 (right) shows that the hydrogen percentage decreases for both cases as more native gas (methane) is produced over time. However, the hydrogen percentage is higher when the CH4 lift table (yellow lines) is used. This can be explained by the pressure plot in Fig. 3, where less gas is being produced as the system is constrained by minimum WHP of 100 psi; that is, the reservoir is depleted less and more hydrogen is available in the vicinity of the well.

This result shows that the lift table has a significant impact when using a standalone model. In practice, a mixture of gases (hydrogen, methane, tiny fraction of the other gases) is produced. In the beginning, the produced gas is pure hydrogen which gradually decreases over time while the composition of other gases increases. Utilizing individual lift tables alone (H2 or CH4) cannot describe the production system accurately. This can only be modeled by a fully integrated model, which captures compositional changes of the produced fluid over time.

Integrated model with CoFlow: The CoFlow module is used to accurately couple the reservoir-wellbore production system. It was already demonstrated that a standalone model with a lift curve of either 100% methane or 100% hydrogen is unrealistic.

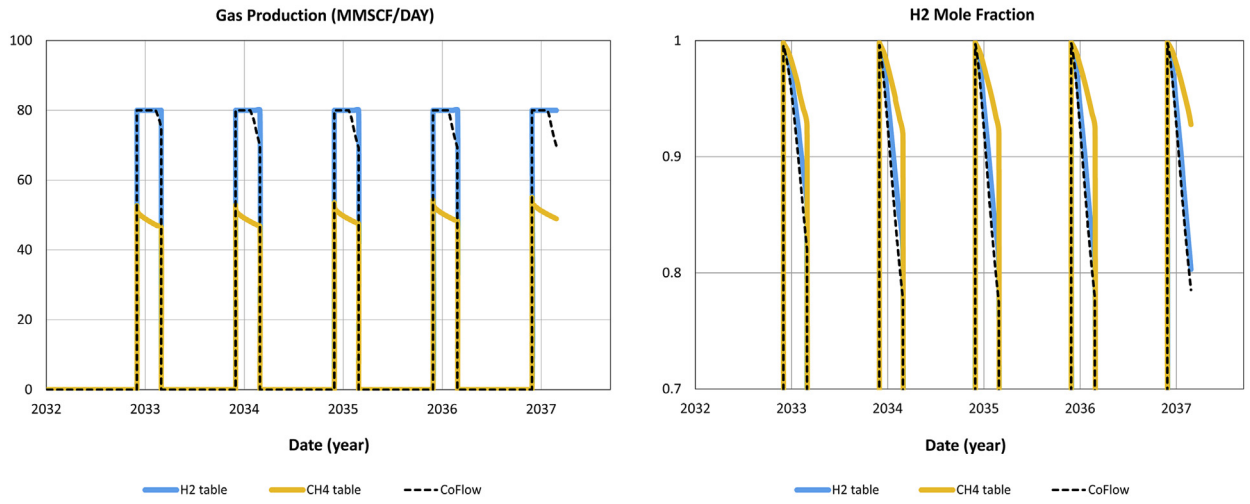

Fig. 2 – Total gas production profile (left) and hydrogen mole fraction (right) in the produced stream for the standalone model with H2 lift table (blue), CH4 lift table (yellow), and CoFlow (black). (For interpretation of the references to colour in this figure legend, the reader is referred to the Web version of this article.)

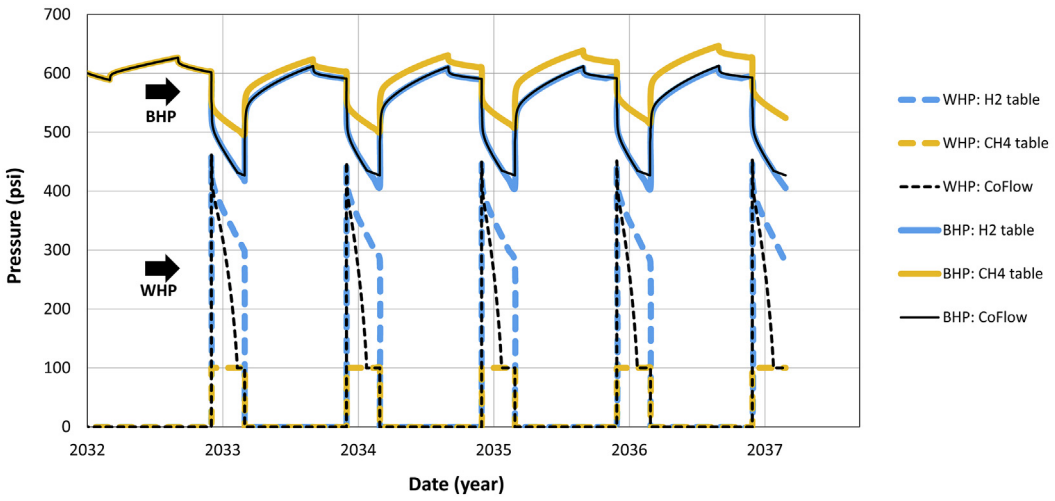

Fig. 3 – Well-head pressure (dashed lines) and bottom-hole pressure (solid lines) for well W01 with H2 lift table (blue), CH4 lift table (yellow), and CoFlow (black). (For interpretation of the references to colour in this figure legend, the reader is referred to the Web version of this article.)

Due to the nature of UHS, the producing gas changes over time, and using a lift table with a fixed composition leads to inaccurate results. Fig. 2 (left) includes the results from CoFlow (black dashed lines), which considers the compositional changes for pressure drop calculations in the wellbore against the results of the standalone model. In the flow model, the so-called shaking hand frequency is set daily basis; this means that the rate at which the GEM reservoir model will deliver (shake hand) its data (IPR, composition, and well indices) to the well model is evaluated daily, this will increase the simulation time considerably, but it gives more accurate results. As can be seen, the field cannot produce the aimed target of 40 MMSCF/day/well (i.e., 80 MMSCF/day in total for two wells) for the three months, especially after the first cycle. This means that the initial reservoir pressure is insufficient to support continuous production. Perhaps, a more extended fill-up period and/or higher injection rate is required to achieve the target rate. This effect is much more pronounced in the hydrogen compositional plot in Fig. 2 (right) when the hydrogen mole fraction drops well below 90%, again showing that the reservoir pressure is insufficient before cycling starts. This can be explained by the pressure plot in Fig. 3, where BHP (solid black lines) and WHP (black dashed lines) for the CoFlow are lying between the results of the standalone models, again highlighting that the CoFlow considers the compositional changes for pressure drop calculations in the wellbore instead of using fixed composition in the standalone models.

This should be noted that the composition of the produced fluid significantly impacts BHP and WHP and, consequently, the rate at the end. As can be seen at the beginning of the production cycle, hydrogen purity is high (the gas column is lighter); this implies that the pure hydrogen lift table can describe the production fluid (blue curves); however, as production continues, the impurities increases in the produced gas and more methane are being produced (the gas column is gradually getting heavier) results in up to ~220 psi additional pressure drop for the CoFlow model and moving the production behavior toward the yellow curves (pure methane lift table). The results show that fully integrated model will improve the prediction of the overall production system.

Sensitivity analysis

Here a couple of scenarios are considered to figure out the impact of different factors on the dynamic behavior of the reservoir during hydrogen storage.

Role of cushion gas

For this analysis, the CoFlow module is used to investigate the impact of different cushion gases on the performance of the UHS in the Viking A field; it should be mentioned that all other properties are kept similar to the base case.

Fig. 4 shows the total gas production rates and hydrogen mole fraction in the produced gas stream from 2032 to 2037 end of the fifth cycle, when using the different cushion gases.

It can be concluded that the lighter the cushion gas, the more hydrogen can produce, especially at early cycles. However, the effect of the cushion gas on the production rate diminishes for later cycles. Furthermore, when the reservoir is filled up with hydrogen before cycling, it results in higher hydrogen purity in the production. But again, this is more visible in early cycles and diminishes in later cycles, and in the fifth cycle, almost equal purity for all cases will be obtained. During these scenarios, 53.3 BSCF of gas in total has been injected, of which 16.5 BSCF during the cushion gas/fill-up injection period and 36.8 BSCF of cycling hydrogen. Fig. 5 shows the amount of produced and remaining hydrogen with different cushion gases.

It is shown that when CO2 is used as cushion gas, 40% of the injected hydrogen remains and cannot be produced back, which resembles the worst performance compared to other scenarios. This result shows that only 22% of the cycling hydrogen remains in the reservoir when the reservoir is filled up with hydrogen before cycling starts.

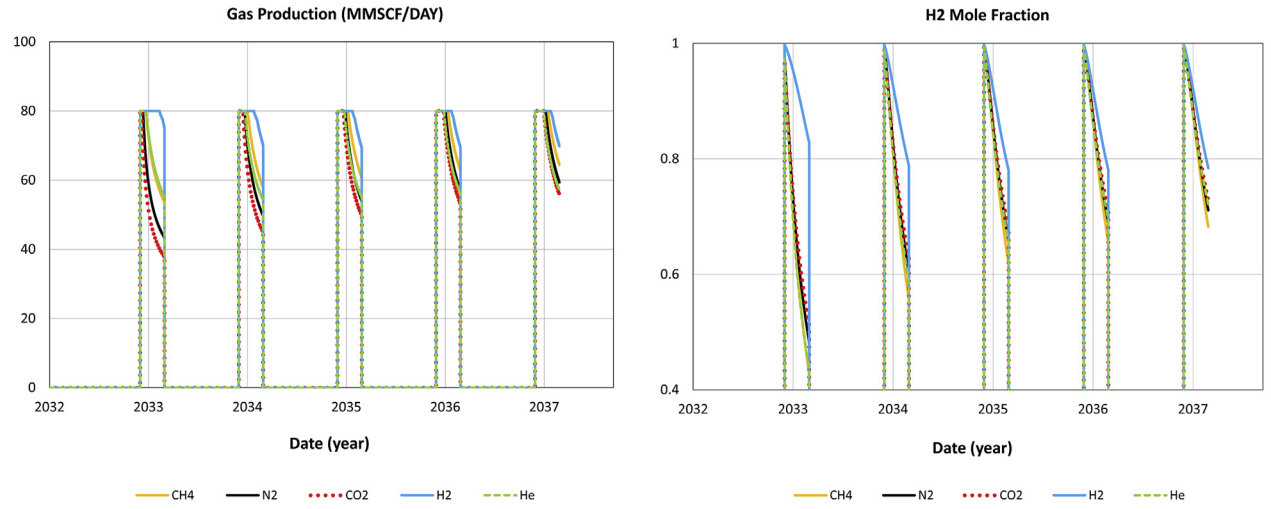

Fig. 4 – Total gas production profile (left) and hydrogen mole fraction (right) in the produced stream using different cushion gases, CH4 (yellow), N2 (black), CO2 (red), H2 (blue), and He (green). (For interpretation of the references to colour in this figure legend, the reader is referred to the Web version of this article.)

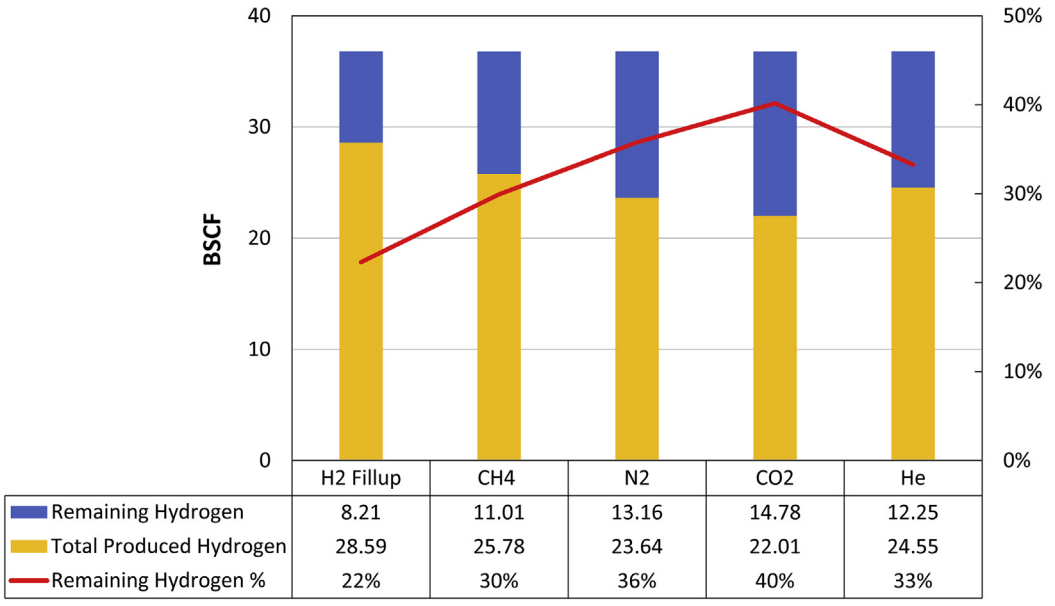

	H2 Fillup	CH4	N2	CO2	He
Remaining Hydrogen	8.21	11.01	13.16	14.78	12.25
Total Produced Hydrogen	28.59	25.78	23.64	22.01	24.55
Remaining Hydrogen %	22%	30%	36%	40%	33%

Fig. 5 – Total produced and remaining hydrogen after five cycles of injection using different cushion gases.

Among other cushion gases, methane performs best, with 30% remaining hydrogen. However, an economic study should be conducted to evaluate the feasibility of such scenarios, as hydrogen is considerably more expensive than other gases. Furthermore, the cost of the separation processes at the surface should also be included in the feasibility study.

Diffusion effect

The hydrogen has very high diffusivity, about 0.61 cm^2/s, almost four times more than methane. Therefore, hydrogen diffusion to the surroundings could affect the project's economy. As the CoFlow simulation with diffusion takes a much longer time, the effect of diffusivity is examined using a standalone GEM simulator with a pure hydrogen lift table. The Sigmund correlation [25] is used to calculate the binary diffusion coefficient between different components in the mixture. Fig. 6 shows the purity of the produced hydrogen and methane with and without the diffusion effect. As expected, hydrogen diffuses into the reservoir and is mixed up with the native fluids (mainly methane) to some extent, producing more methane. However, the level of mixing with the native fluids (i.e., cushion gas) depends on the reservoir properties and cycling strategy [11]. As can be seen, the impact of diffusion is marginal as diffusion is a prolonged process in general that would be more effective

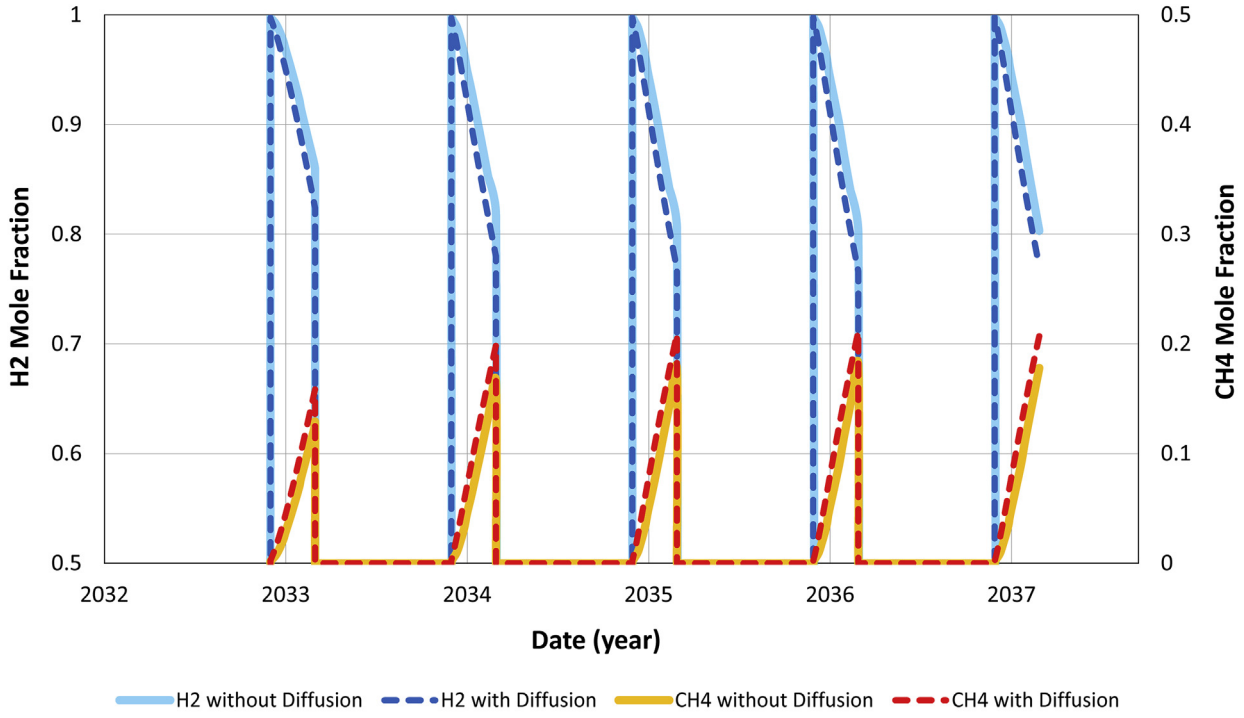

Fig. 6 – Mole fraction of hydrogen and methane without diffusion (solid lines) and with diffusion (dashed lines).

at the time scales beyond the seasonal injection-production intervals.

Extended/longer fill-up period

An important metric to evaluate the performance of the UHS is the purity of the produced hydrogen because this will affect the surface processing operations and, in turn, the operating expenses. To enhance the purity, the fill-up period is extended from 9 months to 2 years with the same rate of 30 MMSCF/day/well of hydrogen (i.e., 60 MMSCF/day in total for two wells), as shown in Fig. 7.

After extending the fill-up period, the reservoir can maintain the target of 40 MMSCF/day/well (i.e., 80 MMSCF/day in total for two wells) for the three-month production period. This is due to the increased BHP compared to the 9-month fill-up period, as shown in Fig. 8. As it can be seen, the purity of produced hydrogen is enhanced to some extent, but a considerable amount of produced methane will still require surface processing.

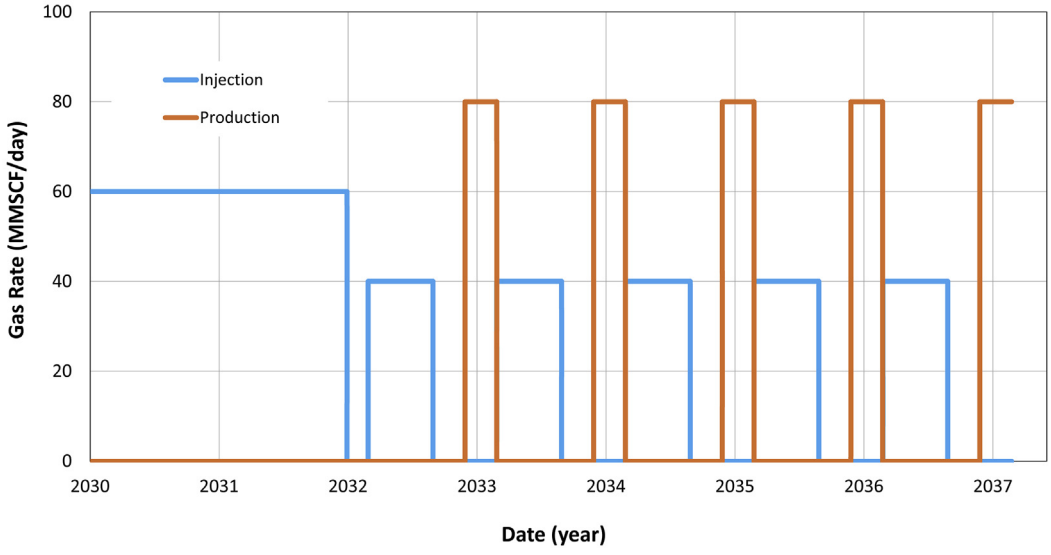

Fig. 7 – Total injection and production profiles with an extended fill-up period (2-year fill-up).

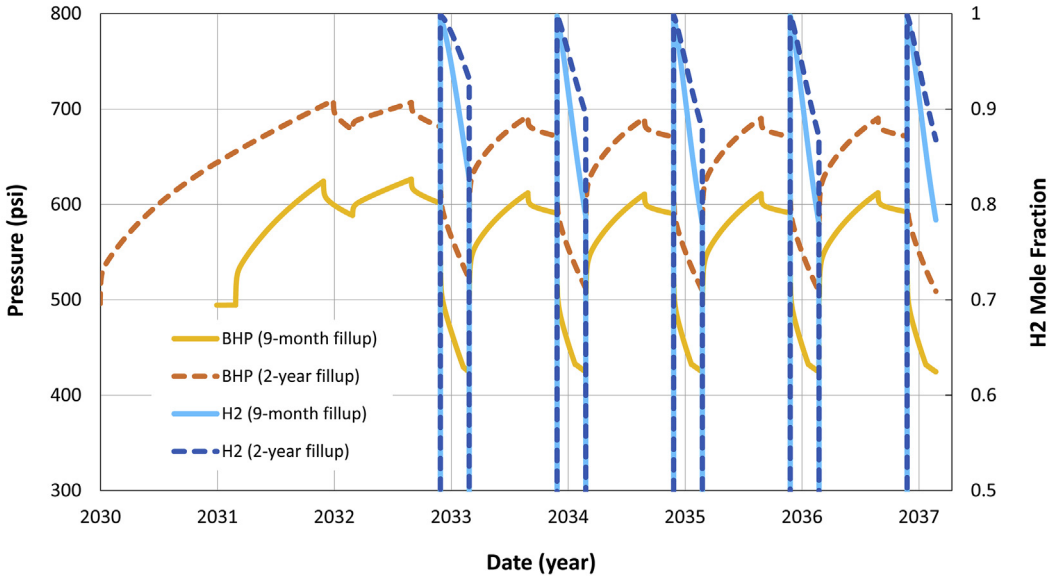

Fig. 8 – Bottom-hole pressure and hydrogen mole fraction of well W01 with 9-month (solid lines) and 2-year (dashed lines) fill-up period.

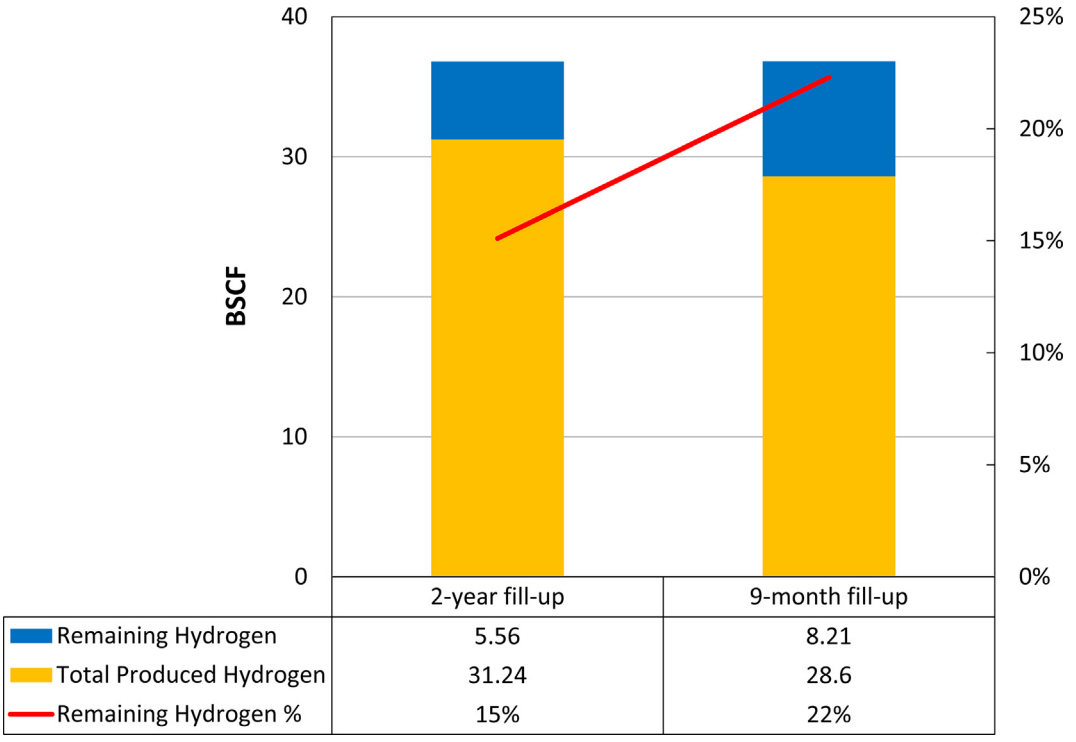

Fig. 9 – Produced and remaining hydrogen with 2-year and 9-month fill-up period.

Fig. 9 shows that, in the 2-year fill-up period, 43.8 BSCF hydrogen is injected vs. 16.5 BSCF in the 9-month fill-up case, and the produced hydrogen is increased only by 9%. This is because the hydrogen dissipates into the reservoir and does not remain in the well's vicinity. Thus, the fill-up hydrogen doesn't act as a good barrier, producing methane.

Increased cycling injection rate

It was shown in Fig. 5 that among different cushion gases other than hydrogen, methane gives the best performance, with the lowest remaining hydrogen of only 30%. Methane, as a cushion gas, has an advantage over hydrogen due to its

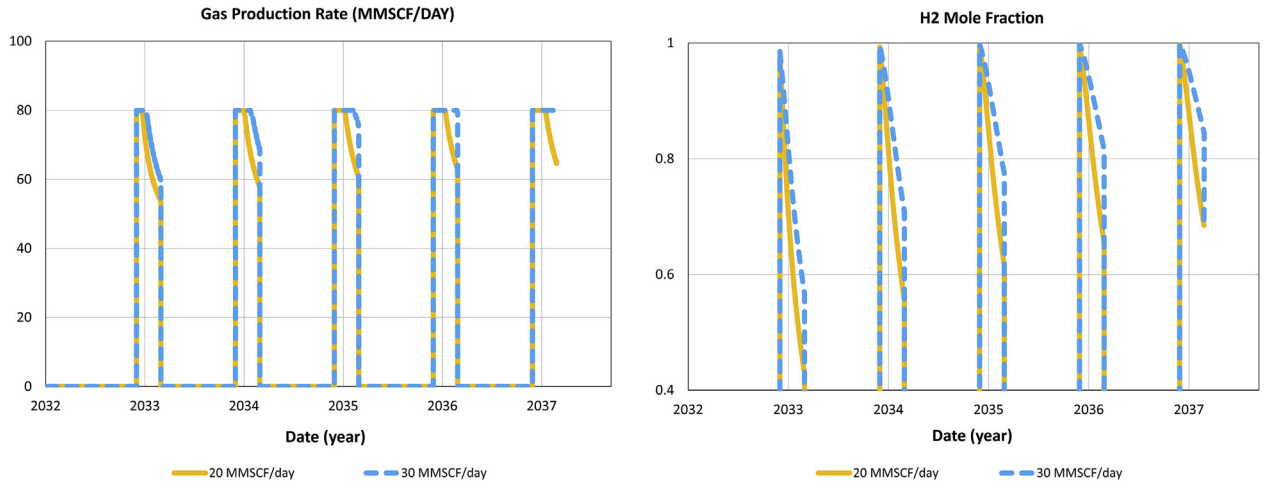

Fig. 10 – Total gas production profile (left) and hydrogen mole fraction (right) in the produced stream with 20 MMSCF/day (solid yellow lines) and 30 MMSCF/day (blue dashed lines) of hydrogen injection. (For interpretation of the references to colour in this figure legend, the reader is referred to the Web version of this article.)

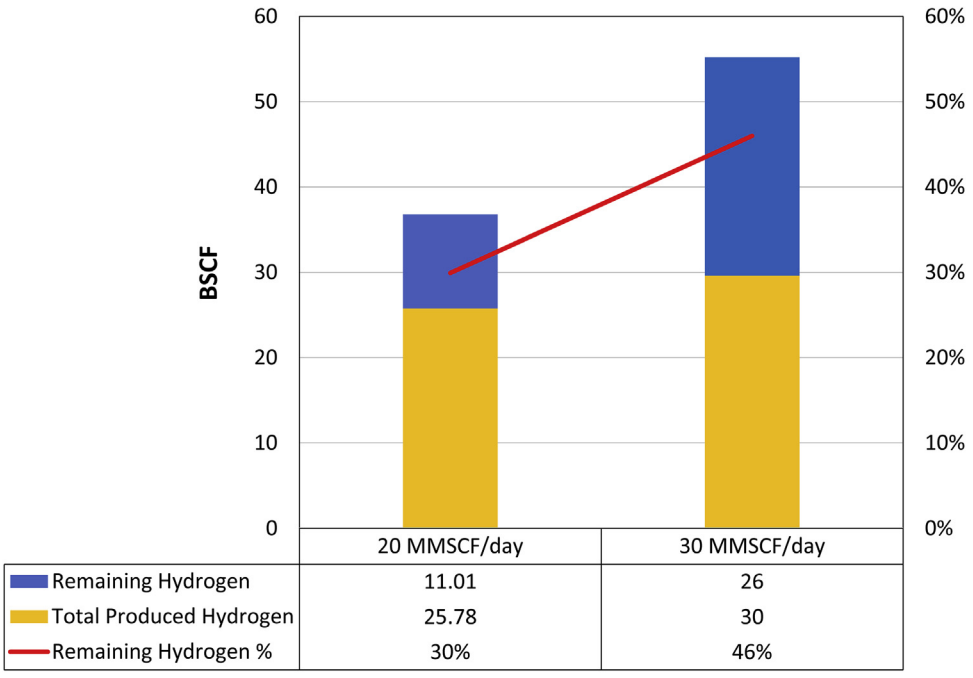

Fig. 11 – Produced and remaining hydrogen with 20 MMSCF/day and 30 MMSCF/day cycling injection rate and methane as cushion gas.

lower cost and availability. Thus, the hydrogen injection rate increases from 20 to 30 MMSCF/day/well in this case.

Fig. 10 shows that the target production rate is reached when the cycling injection rate increases, as more hydrogen is injected than produced; also, the purity of the produced hydrogen increases over time which is more desirable.

Fig. 11 shows that the efficiency is decreased considerably as 46% of the injected hydrogen remains in the reservoir compared to only 30% when injecting at a rate of 20 MMSCF/day.

Conclusions

Through this study, we have shown the role that underground hydrogen storage technology can play in the process of the inevitable energy transition the world needs. Viking A gas field in the North Sea is selected as a potential UHS for that purpose. Our findings are as follows.

- Utilizing the integrated model built with CoFlow, captures the effect of compositional variation of the produced gas

on the vertical flow model. This shows that the integrated model has a significant advantage over a standalone model, especially when the density of components in the produced fluid is considerably different.

- Much care should be given to selecting the cushion gas in terms of density and compatibility compared to the native fluids and the injected hydrogen. It was concluded that the lighter the cushion gas, the more the production rate. Still, the purity of the produced gas will be affected because cushion gas will be produced with hydrogen, which requires further surface processing and increases the total operating cost.
- Hydrogen has high diffusivity compared to methane. The diffusion effect was examined, and the results show that the diffusion effect is marginal.
- The purity of the produced hydrogen is an essential metric for evaluating the UHS performance, efficiency, and, eventually, the project's economics. It was shown that the purity of the produced hydrogen could be enhanced by increasing the fill-up period and the injection rate.

Declaration of competing interest

The authors declare that they have no known competing financial interests or personal relationships that could have appeared to influence the work reported in this paper.

Acknowledgement

The authors gratefully acknowledge Computer Modeling Group (CMG) for providing the CoFlow license for the present work. We also would like to thank Faraj Zarei and Reza Malakooti for their generous and continuous support during the first author's thesis.

REFERENCES

[1] Amid A, Mignard D, Wilkinson M. Seasonal storage of hydrogen in a depleted natural gas reservoir. Int J Hydrogen Energy 2016;41(12):5549–58. https://doi.org/10.1016/j.ijhydene.2016.02.036.

[2] Reuters AP. 4 EU countries pledge tenfold rise in North Sea wind power. In: Deutsche welle, 5/18/2022; 2022. Available online at: https://p.dw.com/p/4BTXq.

[3] Pérez A, Pérez E, Dupraz S, Bolcich J, editors. Patagonia wind - hydrogen project: underground storage and methanation. Spain: World Hydrogen Energy Conference; 2016. 13-16th June 2016. Spain. Available online at: http://www.whec2016.com/.

[4] Arthur TJ. Mesozoic structural evolution of the UK Southern North Sea: insights from analysis of fault systems. PGC 1993;4(1):1269–79. https://doi.org/10.1144/0041269.

[5] European Commission. Directorate general for energy. In: Clean energy for all Europeans. Publications Office; 2019.

[6] Feldmann F, Hagemann B, Ganzer L, Panfilov M. Numerical simulation of hydrodynamic and gas mixing processes in underground hydrogen storages. Environ Earth Sci 2016;75(16):1165. https://doi.org/10.1007/s12665-016-5948-z.

[7] Gray HE. Vertical flow correlation-gas wells. 1978.

[8] Hagemann B, Rasoulzadeh M, Panfilov M, Ganzer L, Reitenbach V. Hydrogenization of underground storage of natural gas: impact of hydrogen on the hydrodynamic and bio-chemical behavior. Comput Geosci 2016;20:595–606. https://doi.org/10.1007/s10596-015-9515-6.

[9] Hassannayebi N, Azizmohammadi S, De Lucia M, Ott H. Underground hydrogen storage: application of geochemical modelling in a case study in the Molasse Basin, Upper Austria. Environ Earth Sci 2019;78(177). https://doi.org/10.1007/s12665-019-8184-5.

[10] Heinemann N, Booth MG, Haszeldine RS, Wilkinson M, Scafidi J, Edlmann K. Hydrogen storage in porous geological formations – onshore play opportunities in the midland valley (Scotland, UK). Int J Hydrogen Energy 2018;43(45):20861–74. https://doi.org/10.1016/j.ijhydene.2018.09.149.

[11] Heinemann N, et al. Enabling large-scale hydrogen storage in porous media – the scientific challenges. Energy Environ Sci 2021;14(2):853–64. https://doi.org/10.1039/D0EE03536J.

[12] Hogeweg S, Strobel G, Hagemann B. Benchmark study for the simulation of underground hydrogen storage operations. Comput Geosci 2022;26:1367–78. https://doi.org/10.1007/s10596-022-10163-5.

[13] Lemieux Alexander, Sharp Karen, Shkarupin Alexi. Preliminary assessment of underground hydrogen storage sites in Ontario, Canada. Int J Hydrogen Energy 2019;44(29):15193–204. https://doi.org/10.1016/j.ijhydene.2019.04.113.

[14] Lysyy Maksim, Fernø Martin, Ersland Geir. Seasonal hydrogen storage in a depleted oil and gas field. Int J Hydrogen Energy 2021;46(49):25160–74. https://doi.org/10.1016/j.ijhydene.2021.05.030.

[15] Navaid HB, et al. A comprehensive literature review on the challenges associated with underground hydrogen storage. Int J Hydrogen Energy 2022. https://doi.org/10.1016/j.ijhydene.2022.11.225.

[16] NSTA Authority. UKCS production. 2022. NSA Authority. UK. Available online at: https://www.nstauthority.co.uk/data-centre/nsta-open-data/production/.

[17] Okoroafor Esuru Rita, Saltzer Sarah D, Kovscek Anthony R. Toward underground hydrogen storage in porous media: reservoir engineering insights. Int J Hydrogen Energy 2022;47(79):33781–802. https://doi.org/10.1016/j.ijhydene.2022.07.239.

[18] Pale Blue Dot Energy. Strategic UK CCS storage appraisal project - site 5: viking. With assistance of UK energy research centre energy data centre (UKERC EDC), pale blue dot. Costain: Axis Well Technology; 2017.

[19] Pfeiffer Wolf Tilmann, Bauer Sebastian. Subsurface porous media hydrogen storage – scenario development and simulation. Energy Proc 2015;76:565–72. https://doi.org/10.1016/j.egypro.2015.07.872.

[20] Pörtner, Roberts DC, Tignor M, Poloczanska ES, Mintenbeck K, Alegría A, et al. Climate change 2022: impacts, adaptation, and vulnerability. Contribution of working group II to the sixth assessment report of the intergovernmental Panel on climate change. IPCC. Cambridge University Press; 2022. Available online at: https://www.ipcc.ch/report/ar6/wg2/downloads/report/IPCC_AR6_WGII_FinalDraft_FullReport.pdf.

[21] Raza Arshad, Arif Muhammad, Glatz Guenther, Mahmoud Mohamed, Al Kobaisi, Mohammed, Alafnan Saad, Iglauer Stefan. A holistic overview of underground hydrogen storage: influencing factors, current understanding, and outlook. Fuel 2022;330:125636. https://doi.org/10.1016/j.fuel.2022.125636.

[22] Riches Hugh. The viking field, blocks 49/12a, 49/16, 49/17, UK North Sea. Memoir 2003;20(1):871–80. https://doi.org/10.1144/GSL.MEM.2003.021.01.73.
[23] Hooper Robert J, More Colin. Evaluation of some salt-related overburden structures in the U.K. Southern North Sea. In: Jackson MPA, Roberts DG, Snelson S, editors. Salt tectonics: American association of petroleum geologists; 1995. p. 251–9.
[24] Shi Zhuofan, Jessen Kristian, Tsotsis Theodore T. Impacts of the subsurface storage of natural gas and hydrogen mixtures. Int J Hydrogen Energy 2020;45(15):8757–73. https://doi.org/10.1016/j.ijhydene.2020.01.044.
[25] Sigmund Phillip M. Prediction of molecular diffusion at reservoir conditions. Part 1- measurement and prediction of binary dense gas diffusion coefficients. J Can Petrol Technol 1976;15(2). https://doi.org/10.2118/76-02-05.
[26] Stefano Patruno, William Reid. Chronostratigraphic and structural framework for the Northern North Sea, central North Sea and west of shetlands (UKCS and NCS) (part of the PESGB "structural framework of the North Sea and atlantic margin" - 2017 edition. 2016.
[27] Proceedings/18th world hydrogen energy conference 2010 - WHEC 2010. Proceedings. World hydrogen energy conference (18, 2010, essen). Jülich: forschungszentrum Jülich, Zentralbibliothek (Schriften des Forschungszentrums Jülich : reihe Energie & Umwelt. In: Stolten Detlef, editor; 2010. vol. vol. 78,4). Available online at: http://hdl.handle.net/2128/4325.
[28] Tarkowski Radosław, Czapowski Grzegorz. Salt domes in Poland – potential sites for hydrogen storage in caverns. Int J Hydrogen Energy 2018;43(46):21414–27. https://doi.org/10.1016/j.ijhydene.2018.09.212.
[29] Thaysen E,M, et al. Estimating microbial growth and hydrogen consumption in hydrogen storage in porous media. Renew Sustain Energy Rev 2021;151:111481. https://doi.org/10.1016/j.rser.2021.111481.
[30] Thiyagarajan SR, Emadi H, Hussain A, Patange P, Watson M. A comprehensive review of the mechanisms and efficiency of underground hydrogen storage. J Energy Storage 2022;51:104490. https://doi.org/10.1016/J.EST.2022.104490.
[31] United Nations Framework Convention on Climate Change. The Paris agreement. FCCC/CP/2015/10/Add.1, revised 2018. Source: Paris Climate Change Conference. Available online at: https://unfccc.int/documents/184656; 2016.
[32] van Hoorn B. Structural evolution, timing and tectonic style of the Sole Pit inversion. Tectonophysics 1987;137(1–4):239–84. https://doi.org/10.1016/0040-1951(87)90322-2.
[33] Wang G, Pickup G, Sorbie K, Mackay E. Scaling analysis of hydrogen flow with carbon dioxide cushion gas in subsurface heterogeneous porous media. Int J Hydrogen Energy 2021. https://doi.org/10.1016/j.ijhydene.2021.10.224.
[34] Ziegler PA. Geology and hydrocarbon provinces of the North Sea. Geojournal 1977;1(1). https://doi.org/10.1007/BF00189601.
[35] Zivar Davood, Kumar Sunil, Foroozesh Jalal. Underground hydrogen storage: a comprehensive review. Int J Hydrogen Energy 2021;46(45):23436–62. https://doi.org/10.1016/j.ijhydene.2020.08.138.